ELSEVIER

Hadronic Final States at HERA

Artem Baghdasaryan

Deutsches Elektronen-Synchrotron, Yerevan Physics Institute

Abstract

The hadronic final state in deep-inelastic ep scattering (DIS) is investigated at HERA. Charged particle production is measured as a function of the pseudorapidity and the transverse momentum, thus testing models of hadroproduction. Scaled momentum distributions of K_S^0 and Λ are measured as a functions of the hardscale Q^2 and are used to test predictions based on fragmentation functions. The production of very forward photons and neutrons is also measured, probing hadroproduction from the proton remnant.

Keywords:
2000 MSC: Charged Particle Spectra, Parton-shower, Forward Neutron Production, Forward Photon Production

1. Charged particle spectra

To investigate the cascade dynamics, charged particle densities as a function of transverse momentum and pseudorapidity were measured in semi-inclusive DIS $ep \rightarrow e^{'}hX$ using the H1 detector at DESY at centre-of-mass energies $\sqrt{s_{ep}} = 319\ GeV$ [1] in the kinematic range of low photon virtuality Q^2 ($5 < Q^2 < 100\ GeV^2$) and small Bjorken x ($10^{-4} < x < 10^{-2}$). In order to distinguish hadronisation effects from effects due to parton evolution the measurements are divided into two regions: low p_T^* ($0 < p_T^* < 1\ GeV$, predominantly sensitive to hadronisation effects) and high p_T^* ($1 < p_T^* < 10\ GeV$, predominantly sensitive to parton dynamics). The p_T^* dependence of the charged particle densities is studied in two different pseudorapidity intervals $0 < \eta^* < 1.5$ and $1.5 < \eta^* < 5$, referred to as the "central region" and "current region" respectively. The target region, $\eta^* < 0$, is not accessible in this analysis. In figure 1 the charged particle densities are shown as a function of η^* for $p_T^* < 1\ GeV$ and $1 < p_T^* < 10\ GeV$ with the predictions of the DGLAP-like model RAPGAP, using different PDF sets. In the soft p_T^* region all NLO PDFs (HERAPDF1.0 [2], CTEQ6.6 [3], GRV98NLO [4]) show similar results and predict less particles compared to calculations using the
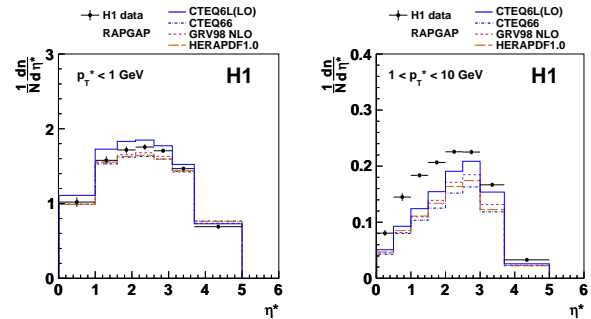

Figure 1: Charged particle density as a function of η^* for $0 < p_T^* < 1\ GeV$ (left) and for $1 < p_T^* < 10\ GeV$ (right), compared to RAPGAP predictions with different proton PDFs.

default LO PDF set CTEQ6L(LO). All predictions are close to the data. At large p_T^* some differences between the NLO PDF sets are observed, with CTEQ6L(LO) being closest to the data, although the differences to the data are still larger than the differences between the various PDF predictions. Similar PDF uncertainties are observed when using the CDM model as implemented in DJANGOH. To check the sensitivity to hadronisation effects, the RAPGAP predictions obtained with three sets of fragmentation parameters (ALEPH tune [5], Pro-
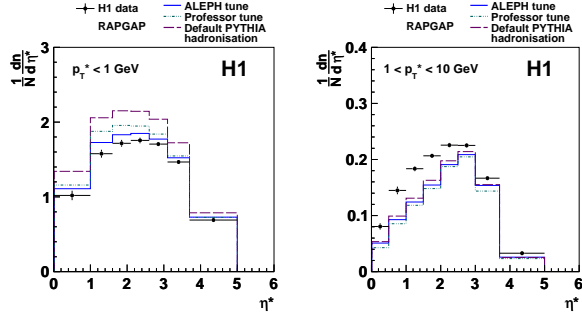
Figure 2: Charged particle density as a function of η^* for $0 < p_T^* < 1\ GeV$ (left) and for $1 < p_T^* < 10\ GeV$ (right), compared to RAPGAP predictions for three different sets of fragmentation parameters.

Figure 3: Charged particle density as a function of η^* for $0 < p_T^* < 1\ GeV$ (left) and for $1 < p_T^* < 10\ GeV$ (right), compared to MCs predictions.

Figure 4: Charged particle density as a function of p_T^* in $0 < \eta^* < 1.5$ (left) and $1.5 < \eta^* < 5$ (right) regions, compared to MCs predictions.

fessor tune [6] and default PYTHIA6.424) are compared to the data in figure 2. Significant differences between these three settings are seen in the soft p_T^* region, where the data are best described by the ALEPH tune. At large transverse momenta they give similar results but none of them describes the data.

In figure 3 the data are compared to different approaches for QCD radiation: the CDM model DJANGOH [7], the DGLAP-based MC RAPGAP [8] and Herwig++ [9] and the CCFM model CASCADE [10]. In the soft p_T^* region DJANGOH and RAPGAP describe the data within the PDF uncertainties. Herwig++, which uses the cluster fragmentation model, provides a reasonable description of the data. CASCADE predicts too high multiplicities in most of the measured range. In the region of $1 < p_T^* < 10\ GeV$ large difference between the predictions are obtained, and the best description of the data is achieved by DJANGOH. RAPGAP strongly undershoots the data in the central region. Herwig++ predicts a spectrum which is even below the prediction of RAPGAP. CASCADE is significantly above the data in a wide range of η^*.

In figure 4 the charged particle densities as a function of p_T^* are shown for two pseudorapidity intervals $0 < \eta^* < 1.5$ (central) and $1.5 < \eta^* < 5$ (current). The shapes of the measured p_T^* distributions in the two pseudorapidity ranges are similar. Predictions based on different parton shower dynamics differ significantly at high p_T^*: RAPGAP and HERWIG++ (DGLAP) strongly undershoots the data not only in the central but also in the current region, DJANGOH (CDM) provides the best description of experimental data in both p_T^* and η^* regions but still not good.

Charged particle production is investigated at H1 also at $\sqrt{s_{ep}} = 225\ GeV$ [11]. At this centre-of-mass energy, using the phase space $5 < Q^2 < 10\ GeV^2$ and

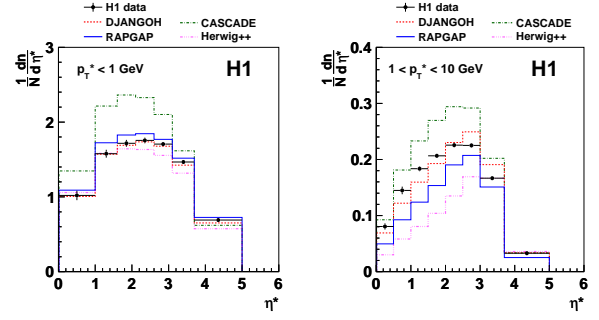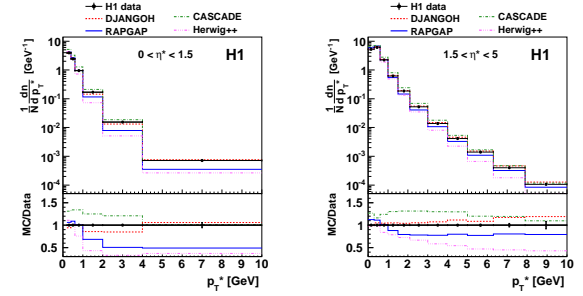$0.35 < y < 0.8$, an improved acceptance and momentum resolutions is achieved for $0 < \eta^* < 3.5$. Cross sections are measured double-differential in η^* and p_T^*. The shape of the cross section as a function of pseudorapidity is modeled well by the DJANGOH and RAPGAP Monte Carlo generators. However, neither Djangoh nor Rapgap describes the charged particle densities as a function of transverse momentum p_T^*, when measured in η^* bins. This confirms the results discussed above.

To study changes in the hadroproduction dynamics along η^*, a phenomenological model is used. This model [12] describes the p_T^* spectrum as the sum of an exponential (Boltzmann-like) and a power-law statistical distribution. It provides a much better description of the data than the often used Hagedorn parameterisation [13]. The relative contribution of the exponential and power-law terms of the model can be characterized by ratio R of the power-law term alone to the total contribution. In figure 5 the relative contribution R of the power-law type distribution to the charged particle production spectra is shown as function of the charged particle rapidity η^*. Close to the virtual photon direction

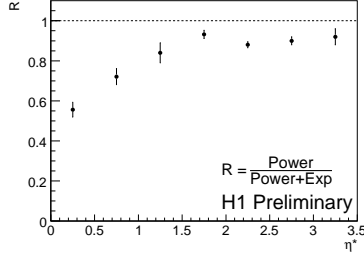(large values of η^*) the p_T^* spectrum can be described

Figure 5: The relative contribution of power-law term.

by a power-law term only, while at central rapidities the data require a significant exponential contribution.

2. Scaled momentum distributions for in DIS

The data most widely used to extract fragmentation functions (FFs) comes from e^+e^- annihilations into charged hadrons. These data are very precise and the predicted cross sections do not depend on PDFs. However, they do not provide information on how to disentangle quark and anti-quark contributions to the FFs and also the gluon fragmentation remains largely unconstrained. For further constraining FFs, scaled momentum distributions, $(1/N)(n(H)/\Delta x_p)$, with $n(H)$ the number of H (K or Λ), N the number of DIS events in a given Q^2 bin and Δx_p the width of the x_p bin, were measured in the current region of the Breit frame [14]. The distributions are presented as functions of Q^2 and scaled momentum x_p ($x_P = 2*P_{Breit}/\sqrt{Q^2}$) in the kinematic region of $10 < Q^2 < 40000\ GeV^2$ and $0.001 < x < 0.75$. Figure 6 shows the scaled momentum distributions for K_S^0 as functions of Q^2 in different regions of x_p. The data show clear scaling violations. This behavior is qualitatively predicted by the parton evolution with increasing Q: the phase space for soft gluon radiation increases, leading to a rise of the number of soft particles with small x_p. The measurements have the potential to constrain significantly the FFs for the strange hadrons K_S^0 and $\Lambda/\bar{\Lambda}$.

3. Forward Neutron and Photon Production in DIS

Forward photon and neutron production cross sections ($\eta^{Lab} > 7.9$) are measured as a function of the energy W of the virtual photon-proton system in HCM in the kinematic range $6 < Q^2 < 100\ GeV^2$ and $0.05 < y < 0.6$ [17]. In Figure 7 normalised to DIS photon and neutron production cross sections as a functions of x_F
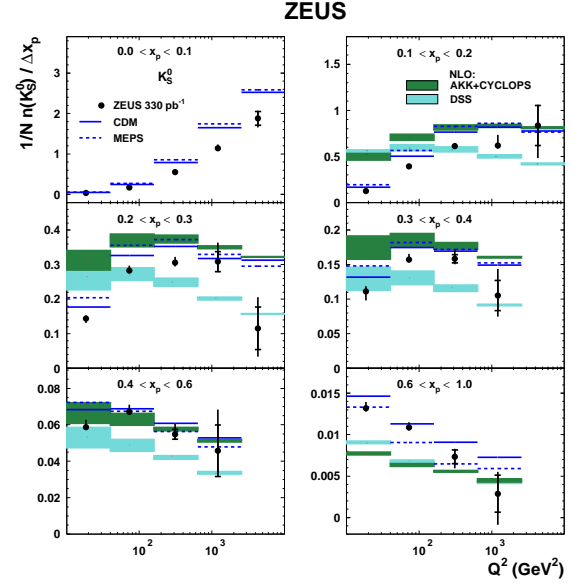

Figure 6: The measured scaled momentum distributions as functions of Q^2 in different regions of x_p (dots). The inner error bars represent the statistical uncertainty. The outer error bars show the statistical and systematic uncertainties added in quadrature. The predictions from CDM [15] (solid lines) and MEPS [16] (dashed lines) are also shown.

in different W intervals are compared to the MC predictions. Photon data are significantly lower than predicted by MC (Data/CDM = 0.6) and neutron data are larger than fragmentation contribution (Data/CDM = 1.35). In Figure 8 the same data are compared to the models of the Cosmic Ray hadronic interactions (CR): EPOS [18], SIBYLL [19], [20] and two versions of QGSJET [21], [22]. Large difference between CR models predictions observed and none of the models describes the photon and neutron data simultaneously. In order to test the Feynman scaling, photon production cross sections at different energy values ($70 < W1 < 130\ GeV$, $130 < W2 < 190\ GeV$, $190 < W3 < 250\ GeV$) are compared. In the figure 9 are shown the cross sections' ratio as well as MCs (upper) and CR models (lower) predictions. The data are consistent with being constant within error, this supporting the hypothesis of Feynman scaling. In contradiction, CR models show W dependence.

4. Conclusion

The charged hadron spectra at low Q^2 and small x are measured in DIS. The data are compared to QCD models with different evolution approaches for simu-
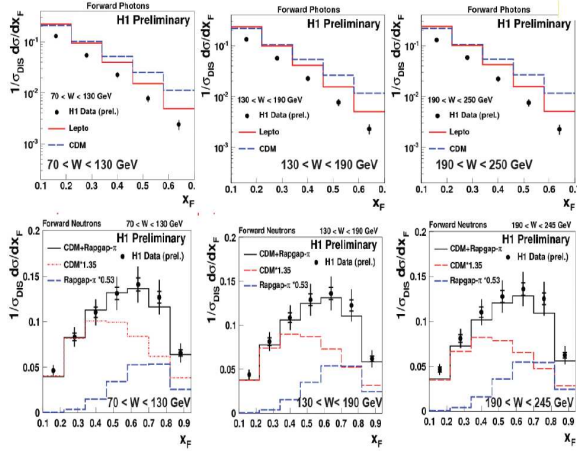
Figure 7: Normalised to DIS photon and neutron production cross sections, compared to MC-s.
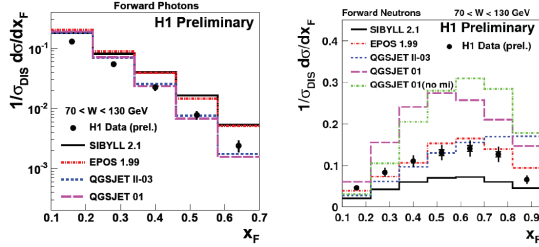

Figure 8: Normalised to DIS photon and neutron production cross sections, compared to hadronic interaction models.

Figure 9: Cross sections ratios at different *W*.

lating the parton cascade and with different hadronisation schemes The Colour Dipole Model implemented in DJANGOH is the best among the other considered MC models and provides a reasonable description of the data, but not good. Phenomenologycal model with a significant exponential contribution in the central region provide a good description of the data.

Scaled momentum distributions for K_S^0 and Λ hadrons are measured for the first time in *ep* DIS. NLO QCD calculations, based on different parametrisations of FFs fail to describe the measurements. The measurements have the potential to constrain significantly the FFs for the strange hadrons K_S^0 and Λ.

Forward photon and neutron production cross sections are measured. The measurements are compared to the MC and Cosmic Ray interaction models. None of the models describes photon and neutron data simultaneously well.

References

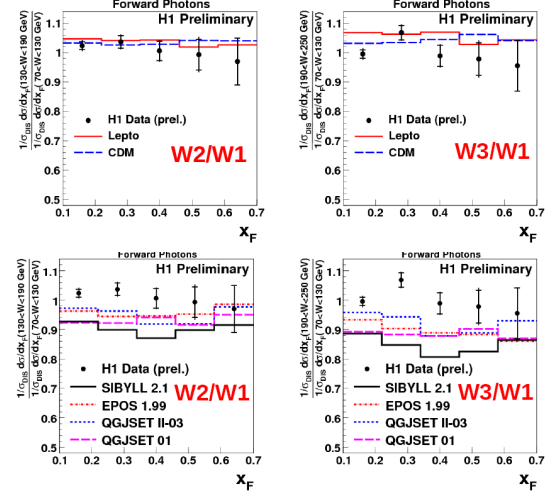[1] C. Alexa et al., H1 Collab., Eur. Phys. J., C73, 02/13, 2406

[2] F. Aaron et al., H1 and ZEUS Collab., JHEP 1001, (2010), 109
[3] P.M. Nadolsky et al., Phys. Rev. D78 (2008) 013004
[4] M. Gluck, E. Reya and A. Vogt, Eur. Phys. J. C5 (1998) 461
[5] S. Schael et al., Phys. Lett. B606 (2005) 265
[6] A. Buckley et al., Eur. Phys. J. C65 (2010) 331
[7] K.Charchula et al., DJANGOH 1.4, Comput.Phys.Commun.81 (1994) 381
[8] H. Jung, RAPGAP 3.1, Comput. Phys. Commun 86 (1995) 147
[9] S. Gieseke et al., Herwig++ 2.5, [arXiv:1102.1672]
[10] H. Jung, Comput. Phys. Commun. 143 (2002) 100
[11] H1 prelim-13-032
[12] A. A. Bylinkin and A. A. Rostovtsev, Phys. Atom. Nucl. 75 (2012) 999
[13] R. Hagedorn, Riv. Nuovo Cim. 6 (1983) 1
[14] H. Abramowicz et al., ZEUS Collab., JHEP 03 (2012) 020
[15] B. Andersson et al., Z. Phys. C 43 (1989) 625
[16] G. Ingelman et al., Comput. Phys. Commun. 101 (1997) 108
[17] H1 prelim-13-012
[18] K.Werner et.al., Phys.Rev. C74 (2006) 044902
[19] J.Engel et al., Phys.Rev. D46 (1992) 5013
[20] E.-J.Ahn et al., Phys.Rev. D80(2009)094003
[21] N.N.Kalmykov et.al., Nucl.Phys.Proc.Suppl.52B (1997) 17
[22] S.S.Ostapchenko, AIP Conf.Proc.928 (2007) 118